A role for the TGFβ-Par6 polarity pathway in breast cancer progression

Alicia M. Viloria-Petit[a], Laurent David[a,1], Jun Yong Jia[a,1], Tuba Erdemir[a], Anita L. Bane[b,c,d], Dushanthi Pinnaduwage[e], Luba Roncari[a], Masahiro Narimatsu[a], Rohit Bose[a,f], Jason Moffat[f], John W. Wong[d,g], Robert S. Kerbel[h,i], Frances P. O'Malley[b,d], Irene L. Andrulis[b,c,d,f], and Jeffrey L. Wrana[a,f,2]

[a]Center for Systems Biology, Samuel Lunenfeld Research Institute, Room 1078 Mount Sinai Hospital, 600 University Avenue, Toronto, ON, Canada M5G 1X5; [b]Department of Pathology and Laboratory Medicine, Mount Sinai Hospital, Toronto, ON, Canada M5G 1X5; [c]Fred A. Litwin Centre for Cancer Genetics, Samuel Lunenfeld Research Institute, Mount Sinai Hospital, Toronto, ON, Canada M5G 1X5; [d]Department of Laboratory Medicine and Pathobiology, University of Toronto, Banting Institute, 100 College Street, Room 110, Toronto, ON, Canada M5G 1L5; [e]Prosserman Centre for Health Research, Samuel Lunenfeld Research Institute, Mount Sinai Hospital, ON, Canada M5G 1X5; [f]Department of Molecular Genetics, 1 King's College Circle, University of Toronto, Toronto, ON, Canada M5S 1A8; [g]Department of Anatomic Pathology, Room E4–32, Sunnybrook Health Sciences Centre, 2075 Bayview Avenue, Toronto, ON, Canada M4N 3M5; [h]Molecular and Cellular Biology, Room S-217, Sunnybrook Health Sciences Centre, Toronto, ON, Canada M4N 3M5; and [i]Department of Medical Biophysics, University of Toronto, Ontario Cancer Institute, Princess Margaret Hospital, 610 University Avenue, Room 7–411, Toronto, ON, Canada M5G 2M9

Communicated by Louis Siminovitch, Mount Sinai Hospital, Toronto, Canada, July 2, 2009 (received for review March 6, 2009)

The role of polarity signaling in cancer metastasis is ill defined. Using two three-dimensional culture models of mammary epithelial cells and an orthotopic mouse model of breast cancer, we reveal that Par6 signaling, which is regulated directly by TGFβ, plays a role in breast cancer metastasis. Interference with Par6 signaling blocked TGFβ-dependent loss of polarity in acini-like structures formed by non-transformed mammary cells grown in three-dimensional structures and suppressed the protrusive morphology of mesenchymal-like invasive mammary tumor cells without rescuing E-cadherin expression. Moreover, blockade of Par6 signaling in an in vivo orthotopic model of metastatic breast cancer induced the formation of ZO-1-positive epithelium-like structures in the primary tumor and suppressed metastasis to the lungs. Analysis of the pathway in tissue microarrays of human breast tumors further revealed that Par6 activation correlated with markers of the basal carcinoma subtype in *BRCA1*-associated tumors. These studies thus reveal a key role for polarity signaling and the control of morphologic transformation in breast cancer metastasis.

epithelial-to-mesenchymal transition | cell polarity | metastasis | tumor invasion | epithelial plasticity

Metastasis, the spread of cancer cells from the primary tumor site to distant organs, accounts for over 90% of deaths in breast cancer patients (1). Metastasis has been associated with epithelial-to-mesenchymal transition (EMT), which is a complex manifestation of epithelial plasticity, in which polarized epithelial cells embedded in organized, stratified, or single cell layers convert into single fibroblastoid cells capable of locomotion (2). Cellular changes necessary for EMT include both morphological changes, as well as alterations in gene expression. While the role of the gene expression program associated with EMT has been well-described (3), it is unclear how the morphological changes associated with EMT specifically contribute to cancer progression and metastasis in vivo. The Par6 polarity complex localizes to the tight junction (TJ) and is an important regulator of the morphological transitions associated with epithelial cell plasticity (4). The complex is comprised of three highly conserved proteins, including Par3, Par6, and aPKC. Par6 is a core component that was initially identified as one of the six Par (for "partitioning"-defective) proteins essential for asymmetric cell division in the *C. elegans* zygote, and was subsequently found to be required for asymmetric division of neuroblasts and the differentiation of oocytes in *Drosophila*, as well as the establishment/maintenance of apical-basal polarity and polarized migration in both *Drosophila* and mammalian cells. Par6-dependent control of apical-basal polarity is mediated by its interaction with Par3 and aPKC, as well as the Crumbs complex (4). Par6 is regulated directly by TGFβ (5) and ErbB-2 receptors (6) to control epithelial cell plasticity and misregulation in expression of polarity proteins, including Scribble and Par6 itself, have been observed to be associated with breast cancer progression (7, 8). However, the role of Par6-mediated signaling in cancer progression has not been well-defined.

Sustained TGFβ receptor signaling has been shown to enhance metastasis in mouse models of breast cancer (1) and in advanced human breast cancer, high TGFβ1 expression has been detected at the invasive leading edge of the tumor (9). In addition, strong associations between tumor levels of TGFβ1 and poor prognosis (1, 10), and between a TGFβ response gene signature and lung metastasis (11), have been observed in patients with breast cancer. Therefore, we used three-dimensional (3D) in vitro cultures of both normal mammary gland epithelial cells and metastatic tumor cells, as well as an orthotopic mouse model of breast cancer to explore the role of TGFβ-polarity signaling in breast cancer progression. We demonstrate that interference with polarity signaling blocks the morphological changes associated with EMT. Furthermore, polarity signaling is critical for the distinctive protrusive morphology of metastatic breast tumor cells and blocking it in vivo suppresses metastasis to the lungs. Moreover, we found that the Par6 pathway was highly active in a subset of human breast tumors with basal subtype features, which are generally more aggressive. These studies thus demonstrate a key role for polarity signaling in breast cancer metastasis.

Results

The importance of the TGFβ-Par6 pathway in breast cancer progression is unknown. Since Par6 is a key component of the core pathways that control apical-basal polarity (4, 6) and there are three Par6 genes (12), RNAi-based approaches were not feasible. We previously used mutant Par6 S345A to block the TGFβ-Par6 pathway (5). Therefore, to evaluate the role of this pathway in breast cancer progression under longer term, more physiologically relevant conditions, we cultured Par6/S345A-

Author contributions: A.M.V.-P., L.D., J.Y.J., T.E., A.L.B., D.P., M.N., R.S.K., F.P.O., I.L.A., and J.L.W. designed research; A.M.V.-P., L.D., J.Y.J., T.E., A.L.B., L.R., M.N., and F.P.O. performed research; A.M.V.-P., L.D., A.L.B., M.N., R.B., J.M., R.S.K., and I.L.A. contributed new reagents/analytic tools; A.M.V.-P., L.D., J.Y.J., T.E., A.L.B., D.P., J.W.W., F.P.O., I.L.A., and J.L.W. analyzed data; and A.M.V.-P., D.P., I.L.A., and J.L.W. wrote the paper.

The authors declare no conflict of interest.

[1]L.D. and J.Y.J. contributed equally to this work.

[2]To whom correspondence should be addressed. E-mail: wrana@mshri.on.ca.

This article contains supporting information online at www.pnas.org/cgi/content/full/0906796106/DCSupplemental.

Downloaded by guest on June 8, 2020

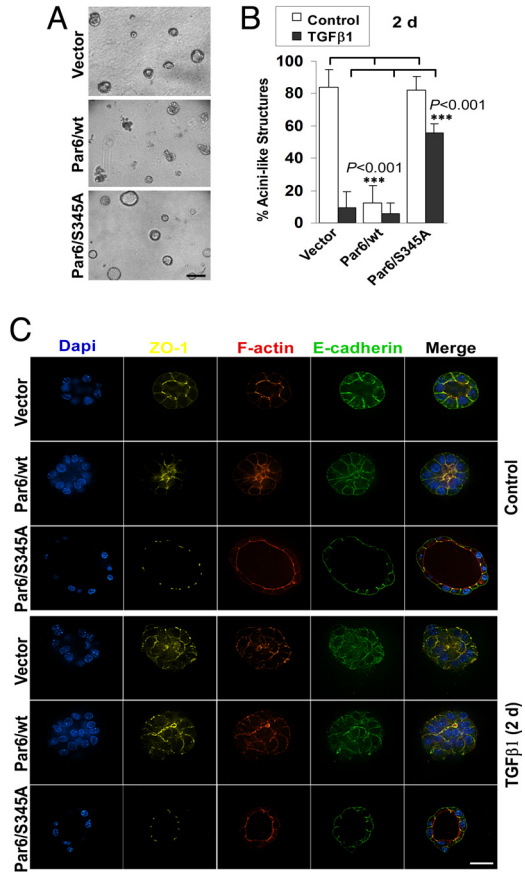


Fig. 1. Activation of the TGFβ-Par6 pathway interferes with the formation of polarized acini-like structures by NMuMG cells. (*A*) Gross morphology of 9-day-old 3D cultures of NMuMG lines expressing empty vector (Vector), wt, or S345A Par6. (*B*) Quantification of acini-like structures. Nine-day-old structures were treated with TGFβ (500 pM; black bars) or without (Control; white bars) for 2 days (2d) and the percentage of acini-like structures (containing a lumen) quantified. Most Par6/wt structures lacked a lumen under basal conditions and maintained their abnormal morphology after TGFβ treatment. In sharp contrast, about 60% of Par6/S345A structures remain polarized after TGFβ exposure. (*C*) The TGFβ-Par6 pathway disrupts polarity in NMuMG 3D structures. TGFβ treated or untreated structures as in *B* were immunostained for nuclei (DAPI, blue) and polarity markers, followed by confocal microscopy analysis. Untreated vector and Par6/S345A structures (*Top*) had well-defined lumens, with ZO-1 (yellow) and F-actin (red) localized to the apical, TJ region, and E-cadherin (green) localized to the AJ, basal to ZO-1. Par6/wt structures had disorganized ZO-1 and F-actin and were lumenless. TGFβ treatment (*Bottom*) caused ZO-1, F-actin, and E-cadherin mislocalization in both Vector and Par6/wt-expressing structures, but not in S345A structures. (Scale bar in *A*, 100 μm; *C*, 20 μm.)

expressing NMuMG cells in 3D cultures using reconstituted basement membrane (Matrigel) (Fig. 1, Fig. S1, and Movie S1). After 9 days in culture, 80% of NMuMG structures were hollow, polarized, and acini-like (Fig. 1 *A* and *B* and Fig. S1) and were characterized by apical ZO-1-, PKC-ζ-, and F-actin-positive tight junctions (TJs); basal-lateral β-catenin- and E-cadherin-positive adherens junctions (AJs); and basal β4-integrin (Fig. S1). Par6/S345A-expressing NMuMG cells were similar to controls (Fig. 1 and Fig. S2). In contrast, 10% or less of the Par6/wt-expressing cells were polarized (Fig. 1*B* and Fig. S2*B*), while the rest were irregular, generally lacked a lumen, and displayed mislocalized ZO-1 and E-cadherin (Fig. 1*C* and Fig. S2*C*). Similar results were obtained using EpH4 mouse mammary epithelial cells (Fig. S3), indicating that disruption of polarity by overexpressed Par6 is not cell-line specific. When 9-day-old NMuMG structures were treated with TGFβ1 for 2 or 6 days (Fig. 1 *B* and *C* and Fig. S2), we observed loss of polarity that was characterized by the loss of the lumen and various markers of epithelial polarity that included apical-lateral ZO-1 and F-actin, and basal-lateral E-cadherin (Fig. 1 *B* and *C* and Fig. S2, respectively). These effects were more pronounced in Par6/wt-expressing structures, consistent with their disturbed acinar morphology in the absence of TGFβ1. In contrast, Par6/S345A structures maintained apical ZO-1, F-actin, lateral E-cadherin, and normal acinar morphology. Thus, TGFβ-treated NMuMG 3D cultures displayed loss of polarity, but not acquisition of complete EMT or protrusive activity. This is likely due to the lack of a transforming oncogene, since previous studies showed that long-term exposure to TGFβ cooperates with oncogenes to promote complete EMT and protrusive behavior in 3D culture conditions (3, 13).

TGFβ-induced loss of expression and lateral localization of E-cadherin and β-catenin is mediated by a Smad-dependent gene expression program [reviewed in (3)]. To confirm that interfering with the TGFβ-Par6 pathway does not significantly impact Smad transcriptional signaling, we examined expression of a panel of 10 TGFβ target genes (14) (Table S1) of known relevance to breast cancer progression. All 10 genes were regulated similarly by TGFβ in Parental, Vector, Par6/wt-, and Par6/S345A-expressing NMuMG cells (Fig. S4*A*). Consistent with this, the anti-proliferative response to TGFβ, which is a well-documented response to Smad signaling (15), was similar in 3D cultures of all three cell types (Fig. S4*B*). Of note, these studies also revealed that overexpression of Par6 (wt or the S345A mutant) induced proliferation, as previously reported for MCF-10A cells (7). We also examined TGFβ-dependent apoptosis in this model, using TUNEL staining. This revealed that 80% of TGFβ1-treated vector or Par6/wt-expressing structures contained apoptotic cells. However, apoptosis was significantly reduced in Par6/S345A-expressing structures (Fig. S4 *C* and *D*), possibly because their highly polarized phenotype confers resistance to apoptosis (16).

Autocrine TGFβ signaling mediates mammary tumor cell migration and breast cancer metastasis in mouse models (17, 18). Therefore, to examine the role of polarity signaling in the context of autocrine TGFβ signaling, we used the EMT-6 mouse mammary carcinoma cell line. EMT-6 cells secrete their own (autocrine) TGFβ, which mediates both their migratory capability ex vivo, as well as their ability to metastasize to the lungs in vivo (17). The cells have undergone EMT, as deduced from their fusiform morphology (19), and they can grow in the mammary fat pad of syngeneic BALB/c mice (i.e., orthotopically). This preserves species-specific interactions between secreted factors and their receptors as well as the host immune response, which is a key target of TGFβ signaling during tumor progression (15). In Matrigel, we observed that EMT-6 cells formed highly protrusive structures with a compact spherical core (Fig. 2*A* and *E*). This morphology was suppressed by a neutralizing TGFβ1 antibody (Ab) (Fig. 2 *A* and *B*), consistent with a key role for autocrine TGFβ in promoting the metastasis of these cells (17). We also examined the human breast cancer line, MDA-MB-231, which is subject to autocrine TGFβ signaling (Fig. S5*A*) that mediates metastasis to lung (20). Like EMT-6, interference with TGFβ suppressed formation of protrusive structures by MDA-MB-231 cells (Fig. S5*B*).

To explore regulation of the Par6 pathway, we next generated an affinity purified rabbit polyclonal phospho-Par6 (pPar6) Ab to Ser 345P, which is phosphorylated by the TGFβ type II receptor (5). Characterization in NMuMG cells revealed robust pPar6 levels in anti-Flag immunoprecipitates (IP) from Par6/wt, but not Par6/S345A-expressing cells (Fig. 2*C*, left blot). Endogenous pPar6 was not detected in NMuMG by IP of total Par6 (Fig. 2*C*, left blot), but it co-precipitated with TGFβRI and was stimulated by TGFβ treatment (Fig. 2*C*, right blot). Further, in

Downloaded by guest on June 8, 2020

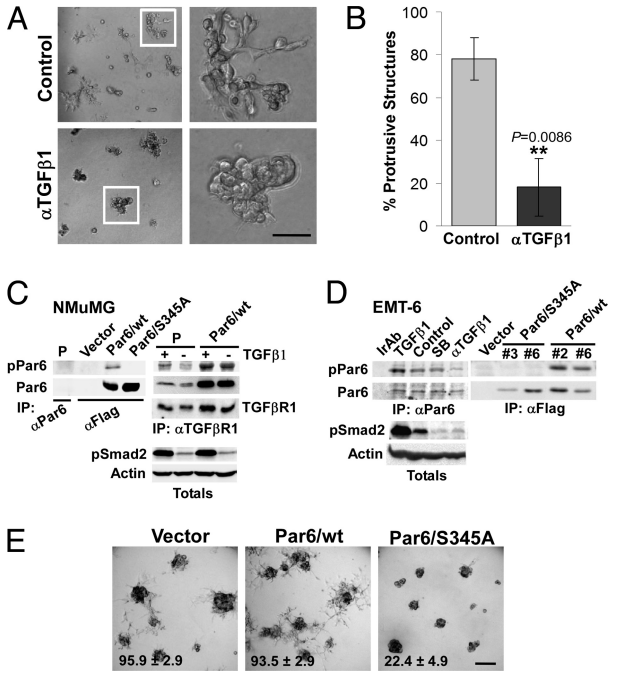


Fig. 2. Autocrine TGFβ signaling regulates the protrusive, mesenchymal phenotype of EMT6 cells via the Par6 pathway. (*A* and *B*) EMT6 cells were grown in Matrigel for 5 days and continuously treated with an anti-TGFβ1 Ab (αTGFβ1) at 10 μg/mL or left untreated, as indicated. Bright field images of 3D structures are shown in *A*, while quantification of protrusive structures formed in control or αTGFβ1-treated cultures is shown in *B*. (*C*) Characterization of a Par6S345P (pPar6) Ab in NMuMG cells. Lysates from parental cells or cells expressing Flag-tagged wt or Par6/S345A were subjected to IP with Abs to Par6 or Flag and immunoblotted for pPar6. A pPar6 band was readily detected in wt but not the Par6/S345A IPs. Endogenous Par6 was not detected in NMuMG parental (*P*) cells after total Par6 IP (*Left*), but co-precipitated with TGFβ receptor I (TGFβRI), in which case TGFβ1 (500 pM, 1.5 h) stimulated Par6 phosphorylation. In Par6/wt overexpressing NMuMG, elevated levels of pPar6 were detected. (*D*) Analysis of endogenous pPar6 in EMT6 cells. Lysates from EMT6 cells subjected to irrelevant Ab IP (Ir Ab) or a Par6 IP were then blotted for pPar6. pPar6 that was present in untreated cells was enhanced by TGFβ1 treatment and was reduced by neutralizing TGFβ Ab (αTGFβ1), but not by 10 μM of the type I kinase inhibitor SB431542 (SB). Lysates were also blotted for pSmad2, which revealed inhibition of autocrine activation by both the neutralizing Ab and SB431542. In the *Right*, phosphorylation of Par6 in wt or Par6/S345A-expressing cells was analyzed by immunoblotting. (*E*) Bright field images of EMT-6 pools expressing empty vector, Par6/wt, or Par6/S345A grown in Matrigel. Quantification of the percent of structures with protrusive morphology (mean +/− SD from three independent experiments shown at the bottom of each image; see *SI Text* for details) shows that Par6/S345A expression significantly suppresses ($P < 0.005$) the percent of protrusive structures formed by EMT-6 cells. (Scale bar in *A*, 50 μm; *E*, 100 μm.)

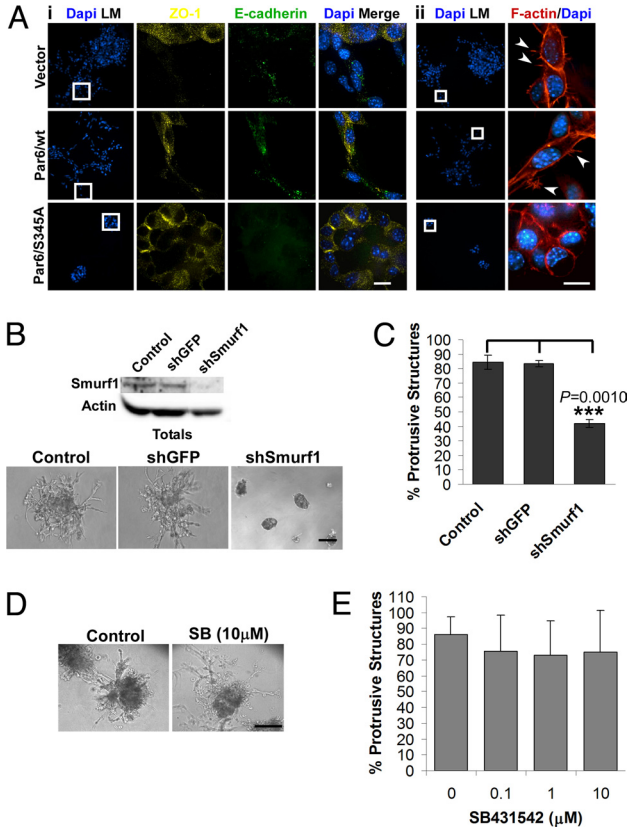


Fig. 3. Par6 phosphorylation mediates morphologic EMT via Smurf1. (*A*) IF and confocal microscopy analysis of EMT-6 3D structures. (*i*) Selected areas of the lower magnification (white box, Dapi LM column) image are shown to the right with the ZO-1 (yellow), E-cadherin (green), and the merged image (Dapi merge) stains. Both Vector and Par6/wt structures showed only cytoplasmic ZO-1. In contrast, Par6/S345A structures showed membrane ZO-1 staining and luminal space. E-cadherin was poorly expressed in all structures, particularly in those formed by S345A cells. (*ii*) F-actin staining showed distinctive filopodial and lamellipodial-like protrusions (white arrows) in Vector and Par6/wt structures that were absent in Par6/S345A structures. (*B* and *C*) Smurf1 knockdown blocks protrusive structures in EMT-6 cells. Pools of EMT6 cells transduced with empty vector (control), or expression of shRNA to GFP (shGFP) or Smurf1 (shSmurf1) were analyzed for steady-state Smurf1 protein (*Top*) and grown in 3D cultures (bright field images, *Bottom*). Note suppression of protrusive structures by Smurf1 knockdown that is quantitated in *C*. (*D* and *E*) SB431542 treatment of EMT-6 3D cultures does not interfere with protrusive structures. EMT6 cells grown in 3D cultures were treated with DMSO or the indicated concentrations of SB431542 continuously for 11 days. Quantitation of protrusive structures is shown in *E*. (Scale bar in *A*, 16 μm; *B* and *D*, 100 μm.)

cells overexpressing Par6/wt, elevated pPar6 was detected bound to TGFβRI (Fig. 2*C*, right blot). In EMT-6 cells, pPar6 was constitutively present, was enhanced by exogenous TGFβ treatment and anti-TGFβ1 treatment led to down-regulation (Fig. 2*D*, left blot). As expected, the TGFβRI small molecule antagonist, SB431542, had no effect on pPar6, but clearly suppressed phosphorylation of Smad2, which is a TGFβRI substrate (Fig. 2*D*, left blot). Analysis of EMT-6 cells expressing Par6/S345A revealed an absence of Par6 phosphorylation in S345A-expressing cells (Fig. 2*D*, right blot).

Next we analyzed EMT6 cells in 3D cultures. Expression of Par6/S345A had a striking effect on 3D morphology, causing the usually protrusive structures to become spherical and significantly less protrusive (Fig. 2*E*). In contrast, structures formed by cells expressing Par6/wt maintained a protrusive phenotype. Similar observations were made in MDA-MB-231 cells (Fig. S5*C*). Furthermore, a significant proportion of the cells that appeared at the periphery of a small central lumen in EMT-6 Par6/345A 3D structures regained junctional ZO-1 staining ($44\% \pm 7, n = 6$) compared to cytoplasmic ZO-1 in the controls (Fig. 3*Ai*). Analysis of F-actin (Fig. 3*Aii*) further revealed that vector and wt Par6 expressing cells displayed abundant filopodial and lamellipodial-like protrusions (Fig. 3*Aii*, arrows) consistent with their mesenchymal character. These structures were strikingly absent in Par6/S345A-expressing cells. The general morphology of the Par6/S345A structures, the appearance of junctional ZO-1, and the loss of protrusive behavior (Figs. 2*E* and 3*A*) suggest a reversion to a phenotype that displays aspects of epithelial polarity, albeit not the fully polarized morphology of non-transformed epithelium (note the low and cytoplasmic E-cadherin expression in Par6 S345A structures; Fig. 3*Ai*). Finally, to investigate pathways downstream of phospho-Par6, we knocked down Smurf1, an ubiquitin ligase effector of the

Downloaded by guest on June 8, 2020

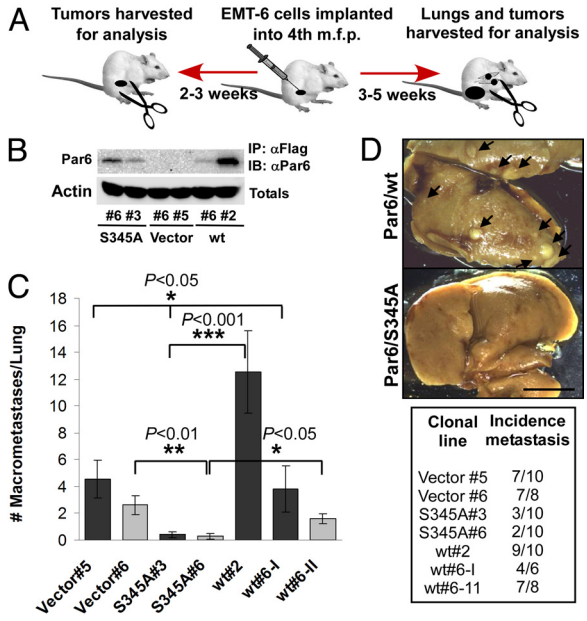


Fig. 4. Par6/S345A suppresses lung metastasis of EMT-6 mammary tumors. (*A*) Diagrammatic representation of the orthotopic model used. m.f.p.: mammary fat pad. (*B*) Relative basal expression of Flag-tagged Par6 in cells implanted into the m.f.p. of BALB/c mice as determined by Flag IP followed by Par6 IB. (*C*) A significant reduction in the number of macroscopic lung metastases was observed in both S345A#3 and S345A#6 tumor bearing mice when compared to mice implanted with either Vector control or Par6 wt tumors. Each bar shade represents an independent experiment. Plotted values correspond to the mean ± SD for $n = 6–10$ (mice per group). The wt#6 clone was tested in both experiments. (*D*) Macroscopic lung metastases in representative lung samples. Metastases appear as white/light yellow spots on the darker yellow background. The incidence of lung metastasis for experiments (*C*) is summarized in the table. Par6/345A tumors showed reduced incidence of lung metastasis as compared to both Vector and Par6/wt tumors (note that similar results were obtained from another independent experiment shown in Fig. S6*D*). (Scale bar, 5 mm.)

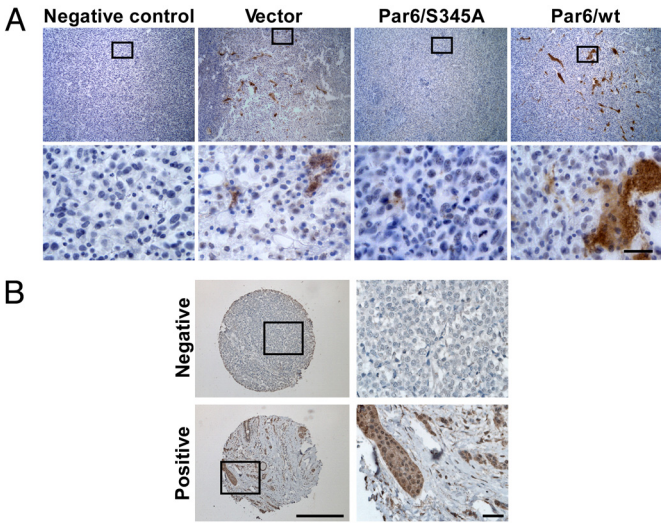


Fig. 5. Immunostaining of pPar6 in mouse and human tumors. (*A*) Analysis of pPar6 in EMT-6 tumors. Tissue derived from syngeneic mouse tumor transplants of the indicated cell lines was stained with pPar6 Ab. Negative control sections were stained in the presence of excess antigen. Note that pPar6 immunoreactivity was present in the cytoplasm and was absent in Par6/S345A expressing tumors. (Scale bar, 100 μM.) (*B*) pPar6 immunostaining in human breast cancer TMAs. Examples of positive and negative staining, as indicated, are shown at lower (left images; scale bar, 500 μm) and at higher magnification (right images, scale bar, 50 μm). pPar6 immunoreactivity was primarily detected in the malignant epithelium, and was typically cytoplasmic, although nuclear immunostaining was occasionally observed. Only cytoplasmic staining was considered for pPar6 scoring (see *SI Text* for details).

pathway (5) (Fig. 3*B*). Loss of Smurf1 expression significantly inhibited the formation of protrusive structures in both EMT-6 (Fig. 3 *B* and *C*) and MDA-MB-231 3D cultures (Fig. S5*D*). Moreover, treatment with SB431542, which blocks Smad signaling, did not block the protrusive morphology of EMT-6 3D structures (Fig. 3 *D* and *E*), indicating that TGFβ's role in promoting EMT-6 protrusiveness is not mediated by the Smad pathway. Taken together, our results demonstrate that the TGFβ-Par6 pathway is activated by autocrine TGFβ in transformed cells and promotes morphological EMT and invasive behavior via the Smurf1 effector.

To analyze metastatic behavior in vivo, we used an orthotopic mouse model. For this purpose, we surgically implanted EMT-6 cells into the right fourth inguinal mammary fat pad of female BALB/c mice and allowed tumors to develop for 3–5 weeks. Animals were then killed and lungs examined for metastases (Fig. 4*A*). Although we observed some variability in tumor take, in neither case did we see significant effects on the growth rate (Fig. S6 *A–C*) of tumors derived from any of the lines tested. However, expression of Par6/S345A in EMT-6 mammary tumors significantly reduced the incidence and number of macroscopic lung metastasis (Fig. 4 *B–D* and another cohort in Fig. S6*D*). In contrast, Par6/wt either had no effect or, in a highly expressing clonal line, increased the number of lung metastases (Fig. 4 *B–D*). To investigate the mechanism by which Par6/S345A inhibited the metastatic spreading of EMT-6 tumors, we next analyzed tumor tissue obtained from 7–14 day old tumors (average size of 0.2 cm^3) using standard IHC and IF. First, using the S345 pPar6 antibody we determined the status of Par6 phosphorylation in Vector, Par6/wt, and S345A tumors. We observed that pPar6 immunostaining of either mouse EMT-6 syngeneic tumors (Fig. 5*A*) or human MDA-MB-231 tumor xenografts (Fig. S5*E*), showed a similar granular cytoplasmic pattern in areas or "patches" of cells that were dispersed throughout the tumor. We confirmed the specificity of the signal by preincubating the primary antibody with a S345 phosphopeptide, which blocked staining (Fig. 5*A*). Positive areas of staining were numerous in EMT-6 Vector (control) tumors and while the frequency of staining was similar in Par6/wt expressing tumors, the intensity of staining was increased. It is unclear why pPar6 activation is sporadic in vivo, but this may be due to mechanisms that restrict TGFβ signaling to the complex, or negative regulatory pathways, such as phosphatases. In stark contrast, pPar6 staining was virtually absent in tumors expressing Par6/S345A (Fig. 5*A*). Thus, Par6/S345A acts as a dominant negative to suppress Par6 phosphorylation in vivo.

IF analyses of Par6/S345A tumors further revealed morphological differences. When we used Flag immunostaining on paraffin sections to specifically identify tumor cells expressing Flag-tagged Par6, round structures formed by Flag-positive cells were readily apparent in Par6/S345A-expressing tumors, but not Par6 wt-expressing tumors (Fig. S7*A*). Dual staining of Flag-Par6 and ZO-1 in tumor cryosections further showed that these Flag-positive structures also stained positive for ZO-1, which was localized to the membrane (compare vector and Par6/S345A tumors in Fig. S7*B*). These structures were not seen in Par6/wt-expressing tumors. Taken together, these results suggest that interfering with Par6 signaling suppresses metastasis and promotes a partial rescue of the epithelial phenotype.

To explore the Par6 pathway in human breast cancer we used a tissue microarray (TMA) from tumors belonging to a cohort that includes patients with hereditary breast cancer. Our previous work revealed high TGFβ levels in *BRCA1*-associated

Downloaded by guest on June 8, 2020

Table 1. Association between pPar6 status and basal cytokeratins/Vimentin in *BRCA1* tumors

	pPar6 Positive (5–8)		pPar6 Negative (1–4)		
Marker	N	%	N	%	P* Value
CK5					
Positive†	17	53.1	15	46.9	
Negative	4	21.1	15	78.9	0.039
CK14					
Positive†	9	75.0	3	25.0	
Negative	10	28.6	25	71.4	0.007
Vimentin					
Positive‡	5	83.3	1	16.7	
Negative	15	35.7	27	64.3	0.069

*P-values from Fisher's Exact Test.
†Positive score (≥ 4) validated by ALB and FPO (Bane AL, et al. (2007) *Am J Surg Pathol* 31 (1):121–128).
‡Positive score (≥ 4) validated by ALB and FPO.

tumors in this cohort (21). Therefore, we analyzed pPar6 levels in this TMA. Using the Allred method (22), pPar6 positivity (Score ≥ 5; Fig. 5*B*) was detected in 42% (122/289) of the breast tumors analyzed (Table S2). Since *BRCA1*-associated tumors are highly enriched in the basal subtype, which is associated with EMT and mesenchymal characteristics (23, 24), we further analyzed pPar6 in the *BRCA1* group. We observed that pPar6 positivity was associated with a subgroup of *BRCA1*-associated breast tumors that displayed basal features; that is, tumors expressing basal rather than luminal cytokeratins. Basal tumors are poorly differentiated invasive carcinomas characterized by, among other features, the expression of cytokeratin (CK) 5/6, 14 and 17, and vimentin (25). We found that basal CK5- and CK14-positive tumors in the *BRCA1*-associated group were more likely to be pPar6 positive than basal cytokeratin negative tumors (53.1% vs. 21.1%; $P = 0.039$ and 75.0% vs. 28.6%; $P = 0.007$, respectively) (Table 1). We also observed that tumors positive for vimentin were more likely to be positive for pPar6, although this correlation was of borderline significance ($P = 0.069$) (Table 1). Associations between pPar6 and basal markers seem to be restricted to the *BRCA1* group, since an additional exploratory study did not detect similar associations in the other groups (Table S3). Survival analysis in all of the patients included showed a clear tendency to reduced overall survival (OS) in pPar6-positive as compared to pPar6-negative patients ($P = 0.067$), particularly after 10 years follow-up (Fig. S8). Taken together, these results support the notion that Par6 phosphorylation is associated with more invasive, metastatic tumors.

Discussion

Our studies have revealed an important role for polarity signaling in mediating loss of cellular polarity and morphologic transformation of mammary cells. Using two 3D culture models of mammary cells that we characterize in this study: NMuMG and EMT-6, as well as previously established 3D culture models that mimic mammary epithelium architecture at various stages of tumor progression, we demonstrated that the TGFβ-Par6 pathway promotes protrusiveness in transformed cells (EMT-6 and MDA-MB-231) that is dependent on the Par6 effector, Smurf1. These findings correlated with in vivo metastatic potential and revealed an in vivo role for polarity signaling in regulating epithelial plasticity within tumors. These studies highlight the relevance of the TGFβ-Par6 pathway to breast cancer invasion and metastasis in an appropriate in vitro and in vivo tissue-like microenvironment.

In NMuMG normal (immortalized) mouse mammary cells, activation of the Par6 pathway interferes with the formation of polarized acinar structures and promotes the formation of lumenless structures. These results are in contrast to the recently reported finding that Par6 overexpression in MCF-10A human mammary cells does not disrupt acinar morphogenesis (7). Nevertheless, we observed that Par6 overexpression also interferes with acini formation and polarization of 3D structures formed by EpH4 mouse mammary cells. This suggests that the effect of Par6 overexpression on 3D morphogenesis may differ among cell types, but is not specific to NMuMG cells. Since the effect of Par6 on polarity is a consequence of its ability to regulate TJ dynamics (5), one possible explanation for this difference is that MCF-10A cells fail to form TJ (26) due to a lack of Crumbs3 expression, which associates with the Par6 complex to mediate TJ formation (27). This suggests that our NMuMG 3D model might be more suitable for EMT studies.

Apart from the direct effects on polarity, two other major cellular outcomes of TGFβ-Par6 signaling were unveiled by our studies of 3D structures, namely its role in TGFβ-induced cell death, and in specifically promoting morphological changes associated with EMT, independent from the gene expression reprogramming induced by the Smad pathway. This report, therefore, describes a regulatory role of the TGFβ-Par6 polarity pathway in mammary cell survival/apoptosis. Since activation of the Par6 pathway causes loss of polarity, while its blockade by the Par6/S345A mutant maintains polarized structures, our results suggest that loss of polarity is a prerequisite for activation of the TGFβ-induced pro-apoptotic cascade. While a detailed molecular understanding of the mechanisms underlying Par6-dependent regulation of apoptosis is beyond the scope of the present study, one previous report has linked β4 integrin-dependent polarity with resistance to apoptosis in 3D structures (16), and the Par6 polarity complex (via aPKC) has been shown to be required for ErbB2/HER-2 dependent survival (28). It will be interesting to test whether modulation of integrin expression or signaling by the Par6/pathway also mediates TGFβ-induced apoptosis.

The pro-apoptotic and EMT-promoting functions of the TGFβ-Par6 pathway in normal and transformed cells, respectively, are consistent with the similar functions of TGFβ itself during tumor progression (29). However, it is of particular note that the Par6 polarity pathway predominantly acts on the TJ complex and is critical for the execution of a program that leads to the cytoskeletal rearrangements required for the morphological events associated with EMT, independent of the canonical TGFβ-Smad pathway and the modulation of AJ. This is a challenging concept, taking into account that the loss of E-cadherin and therefore, the AJ, were believed to be the dominant players in the process of EMT (3). Nevertheless, the importance of the TJ as a target of the TGFβ-Par6 pathway is supported by our analysis of EMT-6 cells, where blockade of Par6 phosphorylation induced morphological mesenchymal-to-epithelial rever-

Downloaded by guest on June 8, 2020

sion and rescues junctional/apical ZO1 ex vivo, without an obvious rescue of E-cadherin expression/localization to AJ. Moreover, in orthotopically implanted EMT-6 mouse mammary tumors, blockade of the Par6 pathway induced the formation of tumor cell derived, ZO-1-positive structures; and significantly reduced the incidence and number of lung metastasis. The good correlation between our in vitro and in vivo results suggests that the EMT-6 3D model might be a reliable in vitro alternative to study the role of TGFβ signaling in breast cancer progression, including testing of signal transduction inhibitors, in an appropriate, tissue-like context.

Our finding of a positive association between the activation status of the Par6 pathway and basal cytokeratins in *BRCA1*-associated tumors suggests that this pathway could be implicated in the aggressive characteristics commonly associated with the basal subgroup of *BRCA1*-associated tumors. It is also possible that TGFβ expression and thus activation of the Par6 pathway may be a molecular event associated with the loss of the *BRCA1* gene, which itself favors a "commitment" to the basal subtype. This hypothesis is further supported by the high TGFβ expression (21) and high incidence of basal carcinoma (30) observed in *BRCA1*-associated tumors. Furthermore, loss of *BRCA1* has been associated with a stem cell-like phenotype (31) and TGFβ signaling in mammary tumor cells is associated with both mesenchymal and stem cell-like properties (32, 33). Detailed molecular analysis and further multivariate studies with human tumor samples are necessary to support this hypothesis.

Materials and Methods

Matrigel 3D Cultures and Immunofluorescence. Cells were maintained under standard culture conditions (see *SI Text*). Subconfluent monolayers were trypsinized, washed, resuspended in assay media, and plated as single cell suspensions on 100% growth factor reduced Matrigel (BD BioSciences) using the overlay method (28). Assay media contained 2% Matrigel added to supplemented mammary media (PromoCell) for NMuMG and MDA-MB-231 cells, or to DMEM plus 2% FBS, 0.5 μg/mL hydrocortisone, 10 μg/mL insulin, and standard antibiotics, for EMT-6 cells. Stable cell lines were cultured with G418. Medium was changed every 3 days. TGFβ1 was added after mature structures were formed. Mouse anti-TGFβ1 or the SB431542 inhibitor was added at the time of plating, and was replenished every 2 days. IF was performed following a standard methodology (28). All IFs were analyzed using a confocal microscope provided with a spinning disk camera (Leica Microsystems). Images were captured and processed using Volocity software (Improvision Inc.). Final images were slices from Z-stacks unless otherwise indicated. For methodologies used to quantify acini-like and protrusive 3D structures see *SI Text*.

EMT-6 Model of Breast Cancer Metastasis. EMT-6 cells were implanted in the mammary gland of BALB/c mice following a reported methodology (17). Tumors were allowed to growth to 1.7 mm^3, at which point mice were euthanized and lungs were harvested for analysis of macrometastases (see *SI Text* for details).

pPar6 Determination in Mammary Tumors. pPar6 expression was assessed in formalin-fixed, paraffin-embedded tissue obtained from mouse or human mammary tumors using an antibody generated during this study. Immunostaining was performed using standard antigen retrieval IHC techniques and a final pPar6 Ab concentration of 2–10 μg/mL. Scoring of pPar6 expression in human TMAs was performed independently by ALB and FPO using the Allred method (22).

For a list of reagents and sources, methodological details and statistical analysis see *SI Text*.

ACKNOWLEDGMENTS. We thank Shan Man (Sunnybrook Health Sciences Centre, Toronto, Canada) for advice on orthotopic surgeries, Susie Tjan (Mount Sinai Hospital, Toronto, Canada) for immunostaining of TMAs, Elizabeth Balogun (Department of Molecular and Cellular Biology, University of Guelph, Canada) for technical assistance, Dr. Martin Oft for the EpH4 cells, Dr. Troy Ketela (Department of Molecular Genetics, University of Toronto, Canada) for help with the design of shRNA viruses, and Drs. Etienne Labbé and Liliana Attisano (Department of Medical Biophysics, University of Toronto, Canada) for PCR primers and a critical review of the manuscript. This work was supported by Canadian Institutes of Health Research (CIHR) and the Canadian Breast Cancer Research Alliance Grant 74692 (to J.L.W.); National Cancer Institute, National Institutes of Health Grant RFA CA-95–011; postdoctoral research awards from Canadian Institutes of Health Research (A.M.V.-P.) and Fondation Pour La Recherche Medicale, France (L.D.); and through cooperative agreements with members of the Breast Cancer Family Registry.

1. Padua D, Massague J (2009) Roles of TGFbeta in metastasis. *Cell Res* 19:89–102.
2. Zavadil J, Bottinger EP (2005) TGF-beta and epithelial-to-mesenchymal transitions. *Oncogene* 24:5764–5774.
3. Huber MA, Kraut N, Beug H (2005) Molecular requirements for epithelial-mesenchymal transition during tumor progression. *Curr Opin Cell Biol* 17:548–558.
4. Bose R, Wrana JL (2006) Regulation of Par6 by extracellular signals. *Curr Opin Cell Biol* 18:206–212.
5. Ozdamar B, et al. (2005) Regulation of the polarity protein Par6 by TGFbeta receptors controls epithelial cell plasticity. *Science* 307:1603–1609.
6. Aranda V, Nolan ME, Muthuswamy SK (2008) Par complex in cancer: A regulator of normal cell polarity joins the dark side. *Oncogene* 27:6878–6887.
7. Nolan ME, et al. (2008) The polarity protein Par6 induces cell proliferation and is overexpressed in breast cancer. *Cancer Res* 68:8201–8209.
8. Zhan L, et al. (2008) Deregulation of scribble promotes mammary tumorigenesis and reveals a role for cell polarity in carcinoma. *Cell* 135:865–878.
9. Dalal BI, Keown PA, Greenberg AH (1993) Immunocytochemical localization of secreted transforming growth factor-beta 1 to the advancing edges of primary tumors and to lymph node metastases of human mammary carcinoma. *Am J Pathol* 143:381–389.
10. Desruisseau S, et al. (2006) Determination of TGFbeta1 protein level in human primary breast cancers and its relationship with survival. *Br J Cancer* 94:239–246.
11. Padua D, et al. (2008) TGFbeta primes breast tumors for lung metastasis seeding through angiopoietin-like 4. *Cell* 133:66–77.
12. Gao L, Macara IG (2004) Isoforms of the polarity protein par6 have distinct functions. *J Biol Chem* 279:41557–41562.
13. Seton-Rogers SE, et al. (2004) Cooperation of the ErbB2 receptor and transforming growth factor beta in induction of migration and invasion in mammary epithelial cells. *Proc Natl Acad Sci USA* 101:1257–1262.
14. Labbe E, et al. (2007) Transcriptional cooperation between the transforming growth factor-beta and Wnt pathways in mammary and intestinal tumorigenesis. *Cancer Res* 67:75–84.
15. Siegel PM, Massague J (2003) Cytostatic and apoptotic actions of TGF-beta in homeostasis and cancer. *Nat Rev Cancer* 3:807–821.
16. Weaver VM, et al. (2002) beta4 integrin-dependent formation of polarized three-dimensional architecture confers resistance to apoptosis in normal and malignant mammary epithelium. *Cancer Cell* 2:205–216.
17. Muraoka RS, et al. (2002) Blockade of TGF-beta inhibits mammary tumor cell viability, migration, and metastases. *J Clin Invest* 109:1551–1559.
18. Muraoka-Cook RS, et al. (2004) Conditional overexpression of active transforming growth factor beta1 in vivo accelerates metastases of transgenic mammary tumors. *Cancer Res* 64:9002–9011.
19. Rockwell SC, Kallman RF, Fajardo LF (1972) Characteristics of a serially transplanted mouse mammary tumor and its tissue-culture-adapted derivative. *J Natl Cancer Inst* 49:735–749.
20. Bandyopadhyay A, et al. (1999) A soluble transforming growth factor beta type III receptor suppresses tumorigenicity and metastasis of human breast cancer MDA-MB-231 cells. *Cancer Res* 59:5041–5046.
21. Bane AL, et al. (2008) Expression profiling of familial breast cancers demonstrates higher expression of FGFR2 in BRCA2-associated tumors. (Translated from Eng) *Breast Cancer Res Treat* (in Eng) [Epub ahead of print].
22. Harvey JM, Clark GM, Osborne CK, Allred DC (1999) Estrogen receptor status by immunohistochemistry is superior to the ligand-binding assay for predicting response to adjuvant endocrine therapy in breast cancer. *J Clin Oncol* 17:1474–1481.
23. Sarrio D, et al. (2008) Epithelial-mesenchymal transition in breast cancer relates to the basal-like phenotype. *Cancer Res* 68:989–997.
24. Mani SA, et al. (2007) Mesenchyme Forkhead 1 (FOXC2) plays a key role in metastasis and is associated with aggressive basal-like breast cancers. *Proc Natl Acad Sci USA* 104:10069–10074.
25. Rakha EA, El-Sayed ME, Reis-Filho J, Ellis IO (2009) Patho-biological aspects of basal-like breast cancer. *Breast Cancer Res Treat* 113:411–422.
26. Underwood JM, et al. (2006) The ultrastructure of MCF-10A acini. *J Cell Physiol* 208:141–148.
27. Fogg VC, Liu CJ, Margolis B (2005) Multiple regions of Crumbs3 are required for tight junction formation in MCF10A cells. *J Cell Sci* 118:2859–2869.
28. Aranda V, et al. (2006) Par6-aPKC uncouples ErbB2 induced disruption of polarized epithelial organization from proliferation control. *Nat Cell Biol* 8:1235–1245.
29. Jakowlew SB (2006) Transforming growth factor-beta in cancer and metastasis. *Cancer Metastasis Rev* 25:435–457.
30. Foulkes WD, et al. (2003) Germline BRCA1 mutations and a basal epithelial phenotype in breast cancer. *J Natl Cancer Inst* 95:1482–1485.
31. Liu S, et al. (2008) BRCA1 regulates human mammary stem/progenitor cell fate. *Proc Natl Acad Sci USA* 105:1680–1685.
32. Shipitsin M, et al. (2007) Molecular definition of breast tumor heterogeneity. *Cancer Cell* 11:259–273.
33. Mani SA, et al. (2008) The epithelial-mesenchymal transition generates cells with properties of stem cells. *Cell* 133:704–715.

Downloaded by guest on June 8, 2020